Published online July 6, 2004

Nucleic Acids Research, 2004, Vol. 32, No. 12 ***3537–3545***
doi:10.1093/nar/gkh683

Reverse gyrase has heat-protective DNA chaperone activity independent of supercoiling

Martin Kampmann* and Daniela Stock

MRC Laboratory of Molecular Biology, Hills Road, Cambridge CB2 2QH, UK

Received March 8, 2004; Revised May 5, 2004; Accepted June 16, 2004

ABSTRACT

Hyperthermophilic organisms must protect their constituent macromolecules from heat-induced degradation. A general mechanism for thermoprotection of DNA in active cells is unknown. We show that reverse gyrase, the only protein that is both specific and common to all hyperthermophiles, reduces the rate of double-stranded DNA breakage ~8-fold at 90°C. This activity does not require ATP hydrolysis and is independent of the positive supercoiling activity of the enzyme. Reverse gyrase has a minor nonspecific effect on the rate of depurination, and a major specific effect on the rate of double-strand breakage. Using electron microscopy, we show that reverse gyrase recognizes nicked DNA and recruits a protein coat to the site of damage through cooperative binding. Analogously to molecular chaperones that assist unfolded proteins, we found that reverse gyrase prevents inappropriate aggregation of denatured DNA regions and promotes correct annealing. We propose a model for a targeted protection mechanism *in vivo* in which reverse gyrase detects damaged DNA and acts as a molecular splint to prevent DNA breakage in the vicinity of the lesion, thus maintaining damaged DNA in a conformation that is amenable to repair.

INTRODUCTION

Hyperthermophilic organisms grow optimally at temperatures >80°C, and some survive >110°C (1). Life under these extreme conditions requires adaptation at the molecular level, since biomolecules are generally not thermostable. Whereas mechanisms of stabilization are known for proteins (2,3), tRNA (4) and membranes (5) of hyperthermophilic cells, a general protective mechanism for DNA is unknown (6).

Heat-induced DNA denaturation is not likely to be a problem of physiological importance: *in vitro*, global strand melting in topologically closed molecules does not occur at temperatures up to 107°C (7). It is the primary structure rather than the secondary structure of DNA that is jeopardized at increased temperature. DNA in aqueous solution is subject to spontaneous hydrolysis of the *N*-glycosyl bond and to cytosine deamination. The rates of these reactions increase exponentially with temperature (8). Base loss, usually depurination, promotes subsequent chain breakage by β-elimination at the 3′ side of the abasic sugar (9). Once a nick has been introduced, the double helical structure is no longer thermostable and strand separation is initiated (7). The rate of depurination in the exposed single-stranded (ss) DNA is 4-fold higher than in double-stranded (ds) DNA (8). Hence, further nicks occur with an increased probability and lead to ds breakage.

Hyperthermophiles must have evolved a way of stabilizing their DNA: the rate of DNA breakage in *Pyrococcus furiosus* at 100°C is 20 times lower than that in *Escherichia coli* at the same temperature (10). Increased salt concentrations afford considerable protection *in vitro* (7), but not all hyperthermophilic cells have high ion concentrations (11). Polyamines and an increased GC-content can stabilize the double helical structure of DNA; however, there is no correlation between these factors and the growth temperature of hyperthermophiles (6,11). Are proteins involved in DNA protection? In heat-resistant bacterial spores, DNA is stored in a partially dehydrated form, packaged by small basic proteins (12). However, such an arrangement is incompatible with DNA replication and transcription in active cells. If proteins protect DNA in hyperthermophiles, they must function in a more dynamic way.

A candidate protein for DNA stabilization is reverse gyrase. The 120 kDa protein has an N-terminal helicase-like domain comprising two RecA folds and a C-terminal domain with homology to bacterial topoisomerase I. It catalyzes the introduction of positive supercoils into DNA (13), and it is thought to be responsible for the occurrence of positively supercoiled plasmids in hyperthermophiles (14). Intriguingly, reverse gyrase is the only protein that is both common and unique to hyperthermophiles (15); it is therefore likely to play a crucial role in thermoadaptation. However, positive supercoiling itself does not protect DNA from thermodegradation, as positively and negatively supercoiled plasmids are equally prone to backbone breaks (7).

We have investigated whether reverse gyrase has protective properties independent of its catalytic activity. Our results indicate that reverse gyrase coats DNA preferentially around nicks, and that this protein coat decreases the rate of backbone breakage. The major effect is not on depurination, but on a later step in the degradation pathway. We propose a possible mechanism in which reverse gyrase stabilizes the DNA backbone at sites of damage and holds DNA fragments together until the damage is repaired by the cellular machinery.

*To whom correspondence should be addressed at present address: The Rockefeller University, 1230 York Avenue, New York, NY 10021, USA. Tel: +1 212 3278101; Fax: +1 212 3277880; Email: Martin.Kampmann@rockefeller.edu

MATERIALS AND METHODS

Proteins

Full-length *Archaeoglobus fulgidus* reverse gyrase was overexpressed in *E.coli* and purified as described elsewhere (16); as detailed there, the protein contained two PCR-induced point mutations, which, however, did not affect protein activity in standard enzymatic assays. Reverse gyrase concentration was measured by the BCA assay (Pierce). Recombinant *Taq* DNA polymerase was a gift from Philipp Holliger (MRC Laboratory of Molecular Biology). Commercial *Taq* DNA polymerase could not be used since glycerol, which is a component of commercial storage buffers, was found to have a heat-protective effect. *Taq* DNA polymerase concentration was estimated from a Coomassie blue-stained polyacrylamide gel, using a BSA standard.

DNA

Plasmid pBR322 was purchased from New England Biolabs and was linearized using EcoRI where indicated. Nicked DNA was obtained by incubating the 1429 bp AatII–BsmI fragment of pBR322 with N.BstNBI nicking endonuclease. All endonucleases were obtained from New England Biolabs. The 1843 bp DNA molecule used in ds breakage assays was synthesized by PCR using KOD polymerase (Novagen) according to the manufacturer's instructions; plasmid pUC19 was used as a template with the following primers: 5′-TGGTTTCTTAGACGTCAGGTGGC-3′ and 5′-GGATAACGCAGGAAAGAACATGTG-3′. The DNA used in the depurination assays was produced in the same way, except that ATP was replaced with 20 μM deoxy[2,8-^{3}H]ATP (24 Ci/mmol; Amersham) in the PCR. PCR products and DNA fragments were purified using a gel purification kit (Qiagen). DNA concentrations were determined by absorbance measurements and/or estimated from agarose gels stained with ethidium bromide.

Thermoprotection assays

DNA solutions contained 1.5 μg/ml DNA, protein as indicated, 20 mM NaCl, 10 mM $MgCl_2$, 2 mM Tris–HCl (pH 8.0) and 1 mM ADP (pH-neutralized) where indicated. In test experiments, the pH of the solution was monitored before and after heat treatment and found to be constant. DNA solutions were overlaid with mineral oil and incubated at 90°C in a thermal cycler (Techne) for the indicated amount of time. For ds breakage assays, proteinase K (Sigma) (to 10 mg/ml) and SDS (to 0.2%, w/v) were added to the samples after the heat treatment and the mixture was incubated at 55°C for 30 min. Under these conditions, reverse gyrase is rapidly degraded (data not shown). The samples were then purified using a PCR purification kit (Qiagen), and 10 μl was subjected to electrophoresis on a 1% agarose gel containing ethidium bromide. The amount of DNA in the band corresponding to the full-length molecule was quantified from the fluorescence intensity using GeneTool software (Syngene). For depurination assays, DNA containing [2,8-^{3}H]adenine was incubated at 90°C as described above. At the indicated timepoints, a 5 μl sample was withdrawn, of which 4 μl was mixed with 0.4 μl of 3 M sodium acetate (pH 5.2) and 13 μl cold ethanol. The sample was stored at −80°C for 30 min. Ethanol-insoluble material was pelleted at 4°C in a microcentrifuge for 10 min at 10 000 rpm. The amount of radiolabel in 13 μl of the supernatant was determined by scintillation counting in FluoranSafe2 buffer (BDH), using a Beckman LS6000 scintillation counter. The total radioactivity per sample was determined before ethanol precipitation. Rate constants were fitted using the Origin software package (Microcal). DNA melting was measured in a sample containing 25 μg/ml of the 1843 bp linear DNA molecule, 20 mM NaCl, 10 mM $MgCl_2$, 2 mM Tris–HCl (pH 8.0), and 375 μg/ml reverse gyrase where indicated. The sample was overlaid with mineral oil in a quartz cuvette and incubated in an oil bath that was heated to increasing temperatures. After temperature equilibration as monitored with a digital thermometer, the optical density (OD) at 260 nm of the sample was determined.

EcoRI cleavage and T7 RNA polymerase transcription

DNA (pGEM-3Z, Promega; at 20 μg/ml) was pre-incubated at 37°C with reverse gyrase or buffer for 3 min at a final concentration of 20 mM NaCl, 16 mM $MgCl_2$, 40 mM Tris–HCl (pH 8.0), 5 mM DTT, 50 ng/μl BSA and nucleotides as detailed. For cleavage reactions, 1 mM ATP was included where indicated; for transcription reactions, 500 μM of ATP, GTP and CTP each were included as well as 100 μM UTP spiked with 2 μCi of [α-^{32}P]UTP (Amersham). After preincubation, EcoRI (New England Biolabs) was added to 100 U/ml or T7 RNA polymerase (USB Corporation) was added to 400 U/ml. For cleavage reactions, 100 μl timepoints were withdrawn and the reaction was stopped by adding 40 μl of cold EDTA (100 mM, pH 7.4). The DNA was purified using a PCR purification kit (Qiagen) and the linearized fraction was quantified on 1% agarose gels stained with ethidium bromide, using GeneTool software (Syngene). For transcription reactions, 5 μl was withdrawn from the mixture and the reaction was stopped by adding 45 μl of cold EDTA (50 mM). Unincorporated nucleotide was removed using Microspin G-25 columns (Amersham), and the amount of radionucleotide incorporated into the high molecular weight fraction was quantified by scintillation counting as described above. The total amount of radioactivity per timepoint was quantified in a sample that had not been purified on Microspin G-25 columns.

Electron microscopy (EM)

DNA (1.5 μg/ml) was incubated at room temperature for 5 min with varying amounts of protein as indicated, at a final concentration of 60 mM NaCl, 10 mM $MgCl_2$, 6 mM Tris–HCl (pH 8.0) and 1 mM ADP or adenylyl imidodiphosphate (ADPNP) where indicated. An aliquot of 0.8 μl of the sample was applied to a carbon-coated EM grid. After 1 min, 10 drops of aqueous uranyl acetate (2%, w/v) were added. The grid was briefly blotted with filter paper (Whatman No. 1) and air-dried. Where indicated, rotary shadowing with platinum was carried out at an angle of 10°. Electron micrographs were taken at a magnification of 20 000 with a Philips 208 transmission electron microscope. Where necessary for analysis, images were printed at a final magnification of 430 000. Distances were measured using an electronic map wheel (Scalex). The fractional lattice saturation θ was calculated from the measured length of the coated or the uncoated DNA region, whichever was more amenable to accurate measurement, and the theoretical total length of the DNA molecule.

RESULTS

Reverse gyrase inhibits thermodegradation of DNA

To investigate the effect of reverse gyrase on the thermodegradation of DNA, plasmid pBR322 was incubated at 90°C for 4 h in the presence of increasing amounts of reverse gyrase (Figure 1A, left panel). In the absence of protein, the DNA is completely degraded under these conditions; the smear visible on overexposed images of the agarose gels represents degradation fragments. When reverse gyrase is present at protein/DNA mass ratios (P/D) of 10 and above, a fraction of the DNA molecules is recovered intact. The proportion of open-circular molecules over supercoiled molecules has increased, indicating that some of the rescued molecules were nicked during the heat treatment or that pre-nicked molecules were preferentially rescued.

Reverse gyrase also protects linear DNA from thermodegradation (Figure 1A, right panel). Furthermore, reverse gyrase prevents aggregation of DNA in the well, presumably by preventing inappropriate interactions between ss DNA regions and assisting correct annealing.

In order to quantify the thermoprotective effect, degradation of linear 1843 bp DNA molecules was monitored over time (Figure 1B). The kinetics of ds break formation were consistent with simple first-order kinetics (Figure 1C). Reverse gyrase present at a protein/DNA mass ratio (P/D) of 40 reduced the rate of ds breakage nearly 8-fold, whereas no protection was seen in the presence of reverse gyrase at P/D < 5. This effect was not unspecific, since a different thermostable DNA-binding protein, *Thermus aquaticus* DNA polymerase (*Taq* DNA polymerase), did not afford protection, but even promoted DNA breakage (Figure 1B–D). ATP had no effect on thermoprotection (data not shown), and the protective effect of reverse gyrase was reduced in the presence of 1 mM ADP (Figure 1D).

To reveal the step of the typical DNA degradation pathway (depurination followed by nicking) that is most significantly slowed down by reverse gyrase, rate measurements were carried out for depurination in the presence and absence of reverse gyrase. Depurination was measured as the release of [2,8-^{3}H]adenine from DNA into the ethanol-soluble fraction. Values for the release rates of guanine are assumed to be the same as the measured values for adenine, since the release rates of adenine and guanine are known to be similar (8). Fitted first-order rate constants for these measurements are shown in Figure 1E. The rate of depurination was somewhat reduced by reverse gyrase, but even more so by *Taq* polymerase. ADP did not significantly modulate the effect of reverse gyrase. Taken together, these results indicate that the effect of reverse gyrase on depurination is likely to be nonspecific.

Since DNA degradation is accelerated in ss DNA (8), a possible mechanism of thermoprotection would be the stabilization of ds DNA. To test whether reverse gyrase has this property, we monitored DNA melting in the presence and absence of the protein (Figure 1F). DNA alone shows cooperative melting at ~80°C. In the presence of reverse gyrase, melting initiates at much lower temperatures and the transition is less cooperative. This finding rules out a mechanism in which reverse gyrase stabilizes ds DNA. A likely explanation for the observed result is that reverse gyrase binds and stabilizes ss DNA regions that occur transiently at temperatures below the overall melting temperature of the whole molecule.

Coat formation by reverse gyrase

Reverse gyrase requires ATP and a topologically closed DNA substrate for its catalytic action. Since the thermoprotective effect of reverse gyrase is seen in the absence of ATP, and with a linear DNA substrate, the underlying mechanism is likely to be structural rather than catalytic. To explore a possible structural basis for heat protection by reverse gyrase, we investigated reverse gyrase–DNA complexes using EM. Reverse gyrase from *Sulfolobus tokodaii* is known to coat DNA under appropriate conditions (17). We corroborated these results for *A.fulgidus* reverse gyrase (Figure 2A). Negatively supercoiled pBR322 DNA (SC) maintained its characteristic plectonemic structure upon coating, whereas linearized pBR322 DNA (LI) usually formed a condensed structure when coated. Occasionally, open-circular plasmids (OC) were observed. Length measurements of coated open-circular plasmids were in good agreement with the theoretical length of the naked DNA. This result indicates that, unlike RecA (18), reverse gyrase did not considerably stretch the DNA upon binding and that extensive wrapping of the DNA around the protein did not occur.

To characterize coat assembly, we analyzed electron micrographs of DNA incubated with increasing concentrations of reverse gyrase; typical images are shown in Figure 2B. In Figure 2C, the fractional lattice saturation θ, i.e. the coated fraction of the DNA, was plotted as a function of the protein concentration. In the absence of nucleotide, the relationship is quasilinear, implying near-stoichiometric binding. The slope of the line indicates that approximately 100 reverse gyrase molecules were required to coat the 4361 bp DNA molecule completely, corresponding to a binding site size of 40–45 bp. This number reflects the average length of all DNA stretches bound by one reverse gyrase molecule; some proteins were bound to more than one DNA helix. (A more detailed analysis of binding patterns is presented in Figure S1.) In the presence of ADP or ADPNP, the affinity of reverse gyrase for DNA was reduced (Figure 2C). The distribution of data points is compatible with sigmoid curves, which are indicative of cooperative binding. Using cluster analysis, we confirmed that binding was also cooperative in the absence of nucleotide (Figure S2).

Selective accessibility of reverse gyrase-coated DNA

To characterize the accessibility of DNA in the presence of a reverse gyrase-coat, linearization of pBR322 with EcoRI restriction endonuclease was monitored (Figure 3A). In the absence of ATP, reverse gyrase at P/D 10 reduced the rate of EcoRI cleavage significantly. However, EcoRI digestion was not significantly inhibited when both reverse gyrase and ATP were present. We also tested whether reverse gyrase-coated DNA is competent for transcription by T7 RNA polymerase, and we found that transcription as monitored by the incorporation of [α-^{32}P]UTP was completely abolished in the presence of reverse gyrase at P/D 10 (Figure 3B).

Reverse gyrase recognizes nicked DNA

The fact that reverse gyrase-coated DNA is not transcription-competent suggests that the enzyme does not form a constitutive shell around the chromosome *in vivo*. Furthermore, reverse gyrase concentrations in living cells are unlikely to be sufficient for the formation of a complete coat. It is however

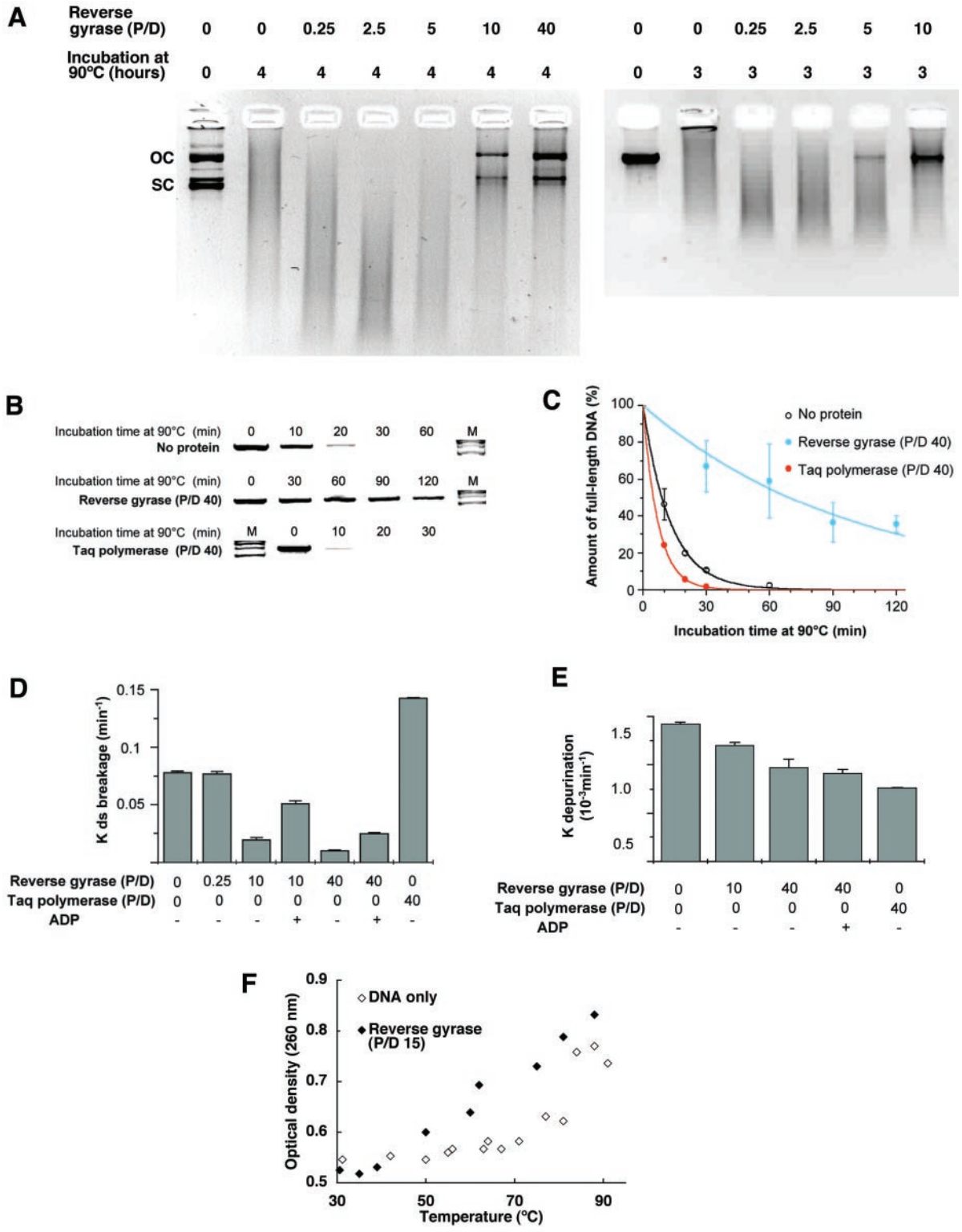

Figure 1. Reverse gyrase inhibits thermodegradation of DNA. (**A**) Plasmid pBR322 (left panel) and a linear 1843 bp DNA molecule (right panel) were incubated at 90°C in the presence of increasing amounts of reverse gyrase. Samples were subjected to electrophoresis on 1% agarose gels stained with ethidium bromide. Images were overexposed to reveal degradation fragments of the DNA. OC, open-circular form and SC, supercoiled form of pBR322. (**B**) Degradation of full-length linear 1843 bp DNA over time was quantified by measuring band intensities. Lanes labeled 'M' contained molecular weight marker; 2500, 2000 and 1500 bp bands are shown. Mean values for 2, 3 and 1 experiment(s) carried out in the absence of protein, in the presence of reverse gyrase (P/D 40) and in the presence of *Taq* DNA polymerase (P/D 40), respectively, are shown in (**C**). Data were fitted to first-order kinetics as indicated by the curves. (**D**) Fitted rate constants for ds breakage are shown for all experimental conditions tested. (**E**) Depurination was measured as the release of [2,8-^{3}H]adenine from ds DNA. Fitted first-order rate constants for depurination are shown for all experimental conditions tested. In (C–E), error bars denote standard errors. (**F**) Melting of the 1843 bp linear DNA molecule was monitored by measuring optical density at 260 nm in the presence and absence of reverse gyrase.

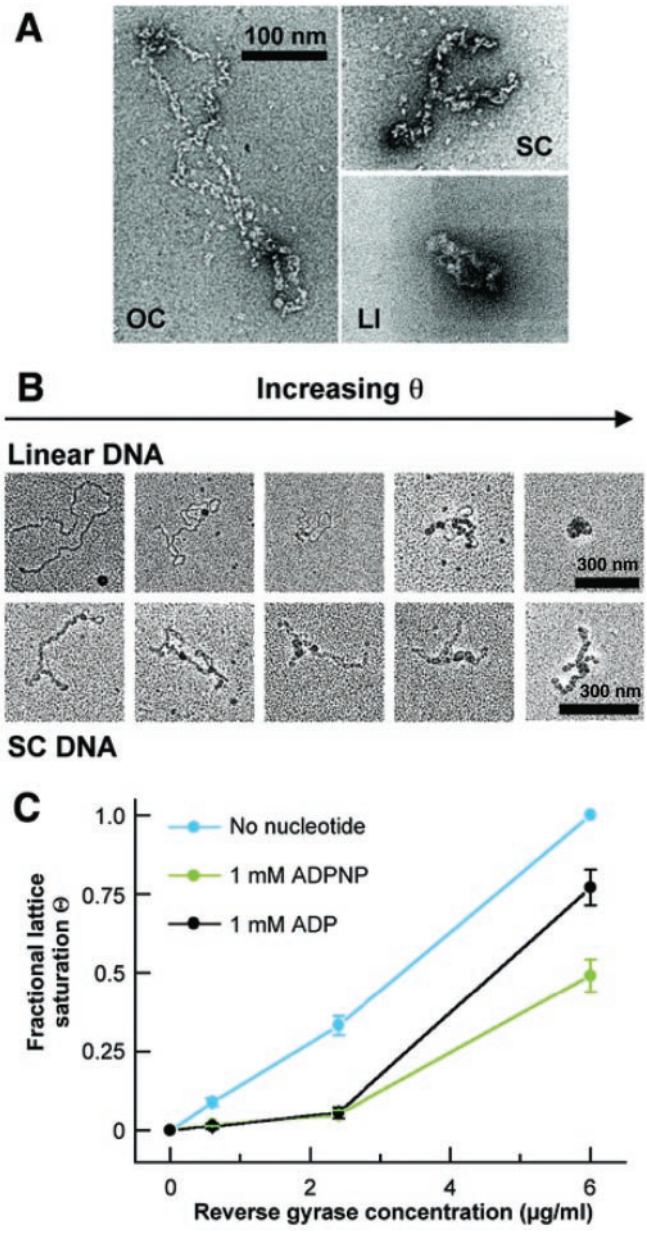

Figure 2. Coat formation by reverse gyrase. (**A**) Electron micrographs of negatively stained complexes of open circular (OC), negatively supercoiled (SC) and linear (LI) pBR322 DNA with excess reverse gyrase. Complexes of linear or supercoiled pBR322 with increasing concentrations of reverse gyrase were imaged by EM after rotary shadowing. Typical electron micrographs are shown in (**B**). The fractional lattice saturation θ, i.e. the fraction of the DNA that was coated with protein, was measured at different protein concentrations and in the absence and presence of nucleotide. Values shown in (**C**) represent means for 16 or more complexes with linear DNA; error bars denote standard errors. Similar results were generally obtained with negatively supercoiled DNA (data not shown).

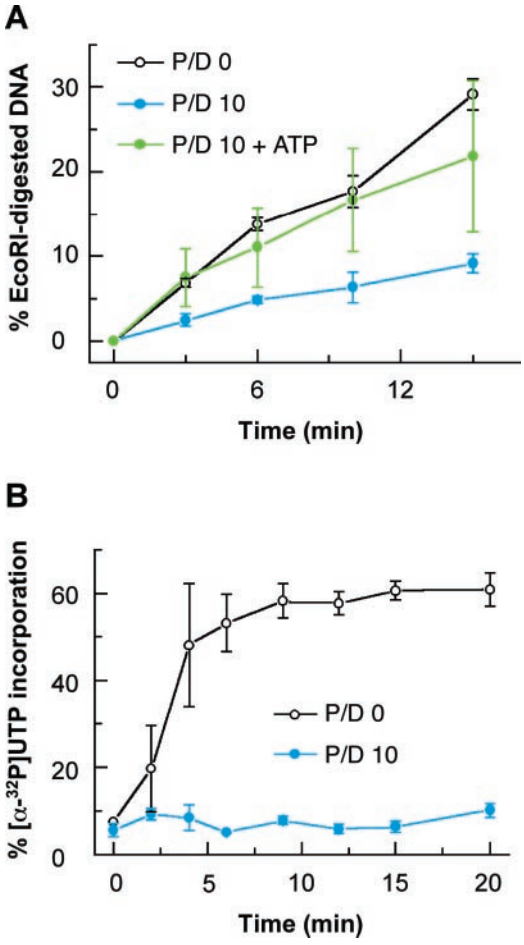

Figure 3. Selective accessibility of reverse gyrase-coated DNA. (**A**) Linearization of pGEM-3Z DNA by EcoRI was monitored by subjecting samples withdrawn at different timepoints to agarose gel electrophoresis and quantifying band intensity. The percentage of linearized DNA was corrected for the presence of linear DNA before EcoRI digestion and plotted against time for reactions carried out in the absence of reverse gyrase (open circles), in the presence of reverse gyrase at P/D 10 (blue circles) and in the presence of both reverse gyrase at P/D 10 and 1 mM ATP (green circles). (**B**) T7 RNA polymerase transcription of supercoiled pGEM-3Z DNA was monitored as the incorporation of [α-^{32}P]UTP into RNA. The results for reactions carried out in the absence (open circles) and presence (blue circles) of reverse gyrase at P/D 10 are shown. In (A and B), mean values from two experiments are shown and error bars denote standard errors.

conceivable that a partial reverse gyrase-coat forms around a site of primary DNA damage. To test whether reverse gyrase binds preferentially to nicked DNA and whether it recruits more protein to adjacent DNA stretches through cooperative binding, we mapped protein-binding sites on nicked and intact DNA as imaged by EM (Figure 4B and E). To obtain an estimate of the accuracy of the measurements, the lengths of 10 linear 1429 bp DNA molecules were determined. The mean value of the measurements was 479 nm (±21 nm, SD), which is in good agreement with the theoretical length of the ds region of 486 nm. A DNA substrate containing a nick in the middle of the molecule was obtained as shown in Figure 4A. The position of the nick can be estimated on electron micrographs, although the two ends of the DNA molecule cannot be distinguished. A binned distribution of the measurements of the length between a bound reverse gyrase molecule and the nearer DNA end is shown in Figure 4C and D. The class width was chosen to be 40.5 nm (~2 SD of the accuracy of measurement determined as described above), corresponding to a DNA segment of 1/12 of the total DNA length.

The distribution of single-protein-binding sites on intact DNA (Figure 4C) is not uniform ($P < 0.05$, χ^2-test); the most distal DNA segment is bound more often than the

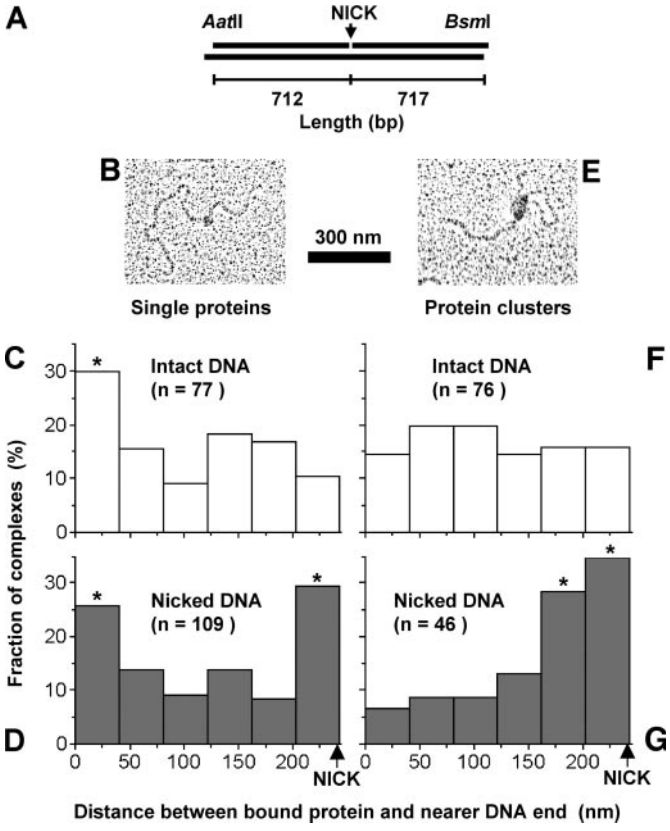

Figure 4. Nick recognition by reverse gyrase. Reverse gyrase molecules in complexes with nicked and intact DNA formed in the absence of nucleotide were imaged by EM after rotary shadowing, as shown in (**B** and **E**). The DNA substrate was the minor AatII–BsmI fragment of pBR322, which contains a single recognition site for the nicking endonuclease N.BstNBI approximately in the middle of the molecule, as illustrated in (**A**). Distances between a bound protein molecule and the nearer DNA end were measured along the DNA contour length. Values were binned as described in the text. Where cluster positions were measured, one count was registered for every bin corresponding to a DNA segment bound by a given cluster. Values marked with an asterisk are significantly higher than values without asterisk (see text for details). (**C**) Positions of single molecules bound to intact DNA. (**D**) Positions of single molecules bound to nicked DNA. (**F**) Positions of protein clusters bound to intact DNA. (**G**) Positions of protein clusters bound to nicked DNA.

other segments. Statistical significance for the increased binding frequency to this segment, and all other values marked with asterisks in Figure 4, was determined as follows: the overall distribution was shown to be significantly different from a uniform distribution (χ^2-test). When the bin of interest was ignored, the remaining distribution was not significantly different from a uniform distribution. Preferential binding of the distal DNA segment reflects an increased affinity of reverse gyrase for DNA ends, which we also observed with other DNA substrates.

With nicked DNA (Figure 4D), the DNA segment containing the nick, as well as the DNA end were bound preferentially. Binding sites of protein clusters were analyzed separately (Figure 4F and G). The cluster distribution on intact DNA (Figure 4F) does not differ significantly from a uniform distribution ($P = 0.88$, χ^2-test). For nicked DNA, however, the nicked segment as well as the segment adjacent to it are preferentially bound (Figure 4G). This result, in conjunction with the finding that reverse gyrase binds DNA cooperatively (Figure 2), suggests that reverse gyrase recruits a protein coat to DNA stretches adjacent to a nick.

DISCUSSION

Possible mechanisms of thermoprotection by reverse gyrase

We have shown that reverse gyrase inhibits thermodegradation of DNA *in vitro*. The thermoprotective activity of reverse gyrase is independent of the positive supercoiling activity of the enzyme: whereas supercoiling requires ATP hydrolysis and topologically closed DNA substrates, we found that linear as well as circular DNA was protected in an ATP-independent way. Thermoprotection required high concentrations of reverse gyrase, implying a structural rather than a catalytic mechanism. Saturation of the thermoprotective effect of reverse gyrase correlates roughly with completion of the protein coat around the DNA.

The typical DNA thermodegradation pathway leading to ds breaks consists of depurination followed by nicking of the weakened backbone (8); once the two DNA strands have been nicked at sites that are sufficiently close together, ds breakage occurs. The effect of reverse gyrase on depurination is small and nonspecific; *Taq* polymerase inhibits depurination more efficiently than reverse gyrase. DNA-binding proteins in general may shield DNA from reactive water molecules by keeping the DNA in a partially desolvated state. The rate of ds DNA breakage however is reduced ~8-fold by reverse gyrase, whereas *Taq* polymerase accelerates ds breakage. The deleterious effect of *Taq* polymerase could be nonspecific; increased rates of chain breakage at apurinic sites in the presence of high concentrations of basic proteins have been reported previously (19).

The results from these kinetic studies indicate that reverse gyrase specifically inhibits one or more steps of the typical thermodegradation pathway that occur after depurination. The effect that reverse gyrase has on DNA melting, as well as the finding that reverse gyrase prevents aggregation of denatured DNA suggest that it stabilizes DNA structures involving ss regions. Two mechanisms are conceivable; they are not mutually exclusive.

First, reverse gyrase may stabilize the DNA backbone at apurinic or ss sites by binding it in a way that is incompatible with the steric requirements of the β-elimination reaction. Backbone stabilization is seen in the crystal structure of a ss octanucleotide in complex with a bacterial type I topoisomerase which is homologous to the C-terminal domain of reverse gyrase. The DNA is held in a conformation typical for B-type DNA, although a complementary strand is not present (20). Such a mechanism would resolve the apparent paradox that reverse gyrase protects DNA from thermodegradation although it can induce DNA denaturation, which should promote degradation: ss DNA bound to reverse gyrase would be at least as stable as ds DNA.

Second, reverse gyrase could clamp repeatedly nicked DNA to prevent the formation of ds breaks by dissociation of the fragments. Thereby, the number of nicks that can be tolerated before ds breakage occurs would be increased. The crystal structure of reverse gyrase shows several extended grooves

and protrusions on the surface of the protein (21) that might bind, clamp and thus stabilize damaged DNA.

Nucleotide-dependent dynamics of the reverse-gyrase coat

The affinity of reverse gyrase for DNA was reduced in the presence of ADP or ADPNP; this is probably why thermoprotection by reverse gyrase was less effective when ADP was present. ATP hydrolysis may therefore drive binding-release cycles, similar to those of molecular chaperones with protein substrates. This idea is supported by the finding that EcoRI access to reverse gyrase-coated DNA is facilitated in the presence of ATP: whereas reverse gyrase binds with high affinity in the absence of nucleotide and consequently inhibits EcoRI cleavage to a significant extent, ATP hydrolysis is likely to promote transient exposure of the DNA stretch containing the EcoRI recognition sequence. Transcription by T7 RNA polymerase was completely abolished by reverse gyrase. The likely explanation for this observation is that transcriptional initiation and elongation requires a long, contiguous region of accessible DNA, whereas DNA coated by reverse gyrase only exposes short, dispersed segments during the binding-release cycles of individual protein molecules.

Possible structural basis for damage sensing

The crystal structure of reverse gyrase (21) has revealed several putative DNA interaction motifs. Intriguingly, a protruding β-hairpin in the N-terminal domain of reverse gyrase is structurally homologous to a β-hairpin that mediates DNA damage sensing in UvrB (22–24), a component of the nucleotide excision repair system. Conserved aromatic residues (Figure 5B) of the hairpin are essential for damage recognition by intercalation (25,26). In *A.fulgidus* reverse gyrase, aromatic residues in corresponding positions (Figure 5A) may fulfill a similar function.

The subtle preference of reverse gyrase for nicked DNA that we found at room temperature may be expected to be much more pronounced at temperatures >80°C, where the structures of nicked and intact DNA differ more dramatically. In particular, partial strand separation adjacent to a nick would expose ss DNA, which is preferentially bound by reverse gyrase [(16) and references therein].

A model for *in vivo* thermoprotection of DNA

Under the experimental *in vitro* conditions, heat protection required the formation of a complete protein coat. However, recruitment of a partial coat to a site of DNA damage occurs at lower concentrations of reverse gyrase, as shown by EM. Hence, reverse gyrase might be expected to provide targeted thermoprotection at physiological concentrations *in vivo*. *In vitro*, DNA damage was not repaired; therefore the number of reverse gyrase molecules available for protection at low protein concentrations would rapidly have been titrated out by the increasing number of damaged DNA sites. *In vivo*, reverse gyrase molecules would no longer be sequestered at the site of DNA damage after repair by the DNA repair machinery, and they could be recruited to other sites of damage. Access of the repair machinery to reverse gyrase-coated DNA may rely on transient release of some reverse gyrase molecules that is controlled by ATP hydrolysis. Such a mechanism would be conceptually similar to sequestration of unfolded proteins by chaperones. It is also possible that reverse gyrase forms part of the DNA repair machinery by recruiting DNA repair enzymes to a lesion analogously to the UvrABC system (25).

It has been suggested that conventional repair systems may be sufficient to protect the DNA of hyperthermophiles from thermodegradation (8). The following argument, as illustrated in Figure 6, supports the need for protection in addition to repair. At 37°C, *in vitro* rates of depurination are very slow, and apurinic sites have a half-life of 190 h before backbone breakage occurs. A second breakage event in the opposite strand can lead to ds breakage if the distance between the two nicks is sufficiently short (Figure 6A). As shown in

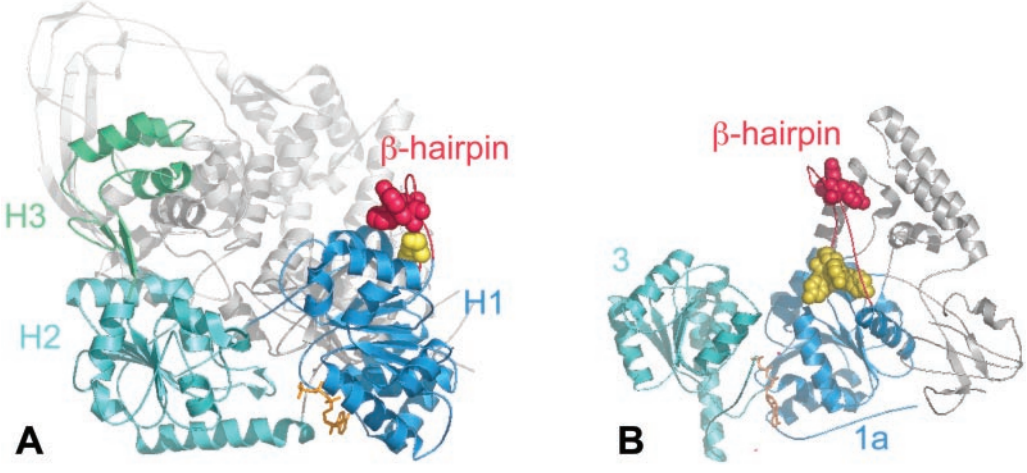

Figure 5. Structural basis for damage recognition. (**A**) Structure of reverse gyrase in complex with ADPNP (PDB code 1GL9). The two RecA folds of the N-terminal helicase domain are colored in blue and cyan, the C-terminal topoisomerase domain is shown in gray, ADPNP in orange and an insertion in the second RecA fold, termed the 'latch' in green. The β-hairpin, which may play a role in DNA damage recognition similar to that of UvrB, is shown in red with aromatic residues highlighted as spheres (Phe-203 in yellow, Tyr-205 and Trp-212 in red). (**B**) Structure of UvrB in complex with ATP (PDB code 1D9Z) in a similar orientation and in corresponding colors. The gray domains are insertions in domain 1a and are postulated to interact with UvrA and UvrC during DNA damage recognition and repair. The aromatic residues in the β-hairpin are highlighted as spheres (Tyr-92, Tyr-93, Tyr-95, Tyr-96 in yellow and Tyr-101 and Phe-108 in red). Details are given in the text. The figure was prepared using the program pymol (http://pymol.sf.net).

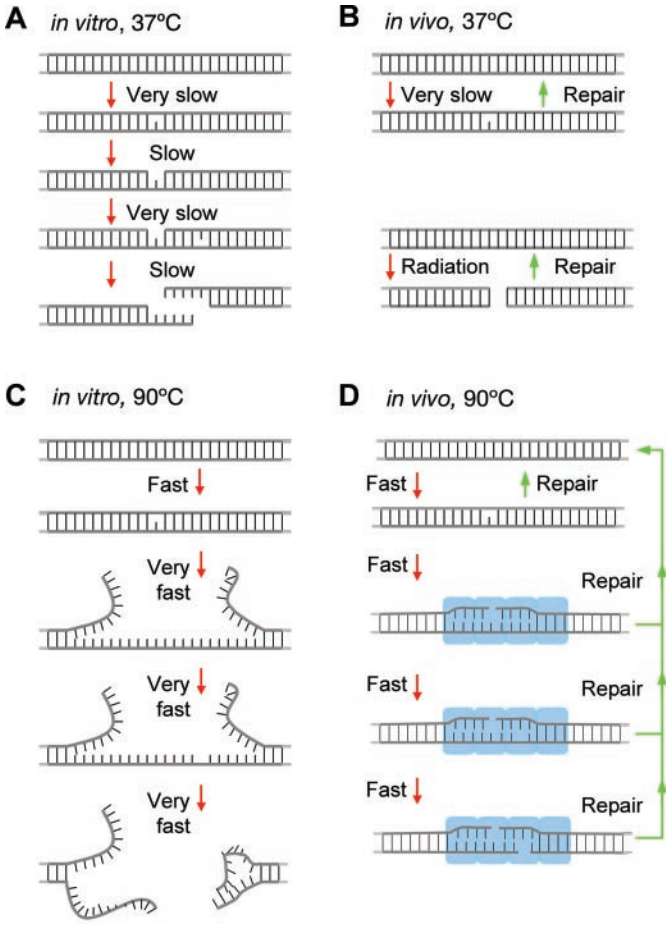

Figure 6. Likely features of spontaneous DNA degradation at different temperatures *in vitro* and *in vivo*. DNA helices represent only a region in a longer molecule. Hydrolysis reactions are indicated by red arrows, enzymatic repair processes by green arrows. Reverse gyrase is drawn as a blue rectangle. A hypothetical model for targeted heat protection by reverse gyrase is shown in (**D**). Details are given in the text.

Figure 6B, apurinic sites are efficiently repaired before backbone breakage occurs *in vivo*, at 37°C (27). Radiation can cause ds breaks, which are repaired by distinct repair systems (28). At 90°C however, the thermodegradation process is not only faster, but also shows qualitative differences (Figure 6C). Once a nick is formed, DNA denaturation is initiated (7). Depurination is accelerated in the exposed ss DNA (8), increasing the probability of a ds breakage. Once a ds breakage has occurred, the fraying DNA ends would form random coils and it is unlikely that conventional repair systems could recognize and process the four disordered, diverging and aggregating strands. As detailed above, two distinct protective functions of reverse gyrase may be envisaged at this stage: backbone stabilization at apurinic sites and, after a backbone breakage event, securing of the DNA ends and possible presentation to the DNA repair machinery. In summary, reverse gyrase might act as a DNA chaperone, which maintains damaged DNA in a structure that is amenable to DNA repair.

A targeted protection mechanism as outlined above would prevent a rare, yet catastrophic event. The results presented in this study indicate that reverse gyrase has properties that would enable it to provide a targeted thermoprotection *in vivo*. Although the primary physiological role of reverse gyrase may be the control of DNA topology (29,30), reverse gyrase could take over protective functions whenever necessary. Proteins that combine isomerase and chaperone functions seem to be a common theme in nature (31). For the first time, we have described topoisomerase and DNA chaperone activity combined in a single enzyme, reverse gyrase.

In yeast, a reverse gyrase-like complex consisting of a topoisomerase and a helicase has been shown to be required for genome stability (32). It is intriguing to speculate that systems analogous to reverse gyrase from hyperthermophiles are involved in DNA protection, damage sensing and repair in mesophilic eukaryotes.

SUPPLEMENTARY MATERIAL

Supplementary Material is available at NAR Online.

ACKNOWLEDGMENTS

We thank Chapin Rodríguez, Andrew Travers, John Rubinstein and Daniela Rhodes for helpful discussions and critical reading of the manuscript, Matthew Higgins and John Berriman for help with EM, and Graeme Mitchison for advice on statistical analysis. M.K. was supported by scholarships from the German Academic Exchange Service (DAAD) and the German National Merit Foundation (Studienstiftung); D.S. was supported by a Medical Research Council Career Development Award.

REFERENCES

1. Stetter,K.O. (1999) Extremophiles and their adaptation to hot environments. *FEBS Lett.*, **452**, 22–25.
2. Szilagyi,A. and Zavodszky,P. (2000) Structural differences between mesophilic, moderately thermophilic and extremely thermophilic protein subunits: results of a comprehensive survey. *Struct. Fold Des.*, **8**, 493–504.
3. Macario,A.J., Lange,M., Ahring,B.K. and De Macario,E.C. (1999) Stress genes and proteins in the archaea. *Microbiol. Mol. Biol. Rev.*, **63**, 923–967.
4. Kowalak,J.A., Dalluge,J.J., McCloskey,J.A. and Stetter,K.O. (1994) The role of posttranscriptional modification in stabilization of transfer RNA from hyperthermophiles. *Biochemistry*, **33**, 7869–7876.
5. Albers,S.V., van de Vossenberg,J.L., Driessen,A.J. and Konings,W.N. (2000) Adaptations of the archaeal cell membrane to heat stress. *Front. Biosci.*, **5**, D813–D820.
6. Grogan,D.W. (1998) Hyperthermophiles and the problem of DNA instability. *Mol. Microbiol.*, **28**, 1043–1049.
7. Marguet,E. and Forterre,P. (1994) DNA stability at temperatures typical for hyperthermophiles. *Nucleic Acids Res.*, **22**, 1681–1686.
8. Lindahl,T. (1993) Instability and decay of the primary structure of DNA. *Nature*, **362**, 709–715.
9. Lindahl,T. and Andersson,A. (1972) Rate of chain breakage at apurinic sites in double-stranded deoxyribonucleic acid. *Biochemistry*, **11**, 3618–3623.
10. Peak,M.J., Robb,F.T. and Peak,J.G. (1995) Extreme resistance to thermally induced DNA backbone breaks in the hyperthermophilic archaeon *Pyrococcus furiosus*. *J. Bacteriol.*, **177**, 6316–6318.
11. Daniel,R.M. and Cowan,D.A. (2000) Biomolecular stability and life at high temperatures. *Cell Mol. Life Sci.*, **57**, 250–264.
12. Setlow,P. (1992) I will survive: protecting and repairing spore DNA. *J. Bacteriol.*, **174**, 2737–2741.
13. Kikuchi,A. and Asai,K. (1984) Reverse gyrase—a topoisomerase which introduces positive superhelical turns into DNA. *Nature*, **309**, 677–681.

14. Declais,A.C., de La Tour,C.B. and Duguet,M. (2001) Reverse gyrases from bacteria and archaea. *Methods Enzymol*., **334**, 146–162.
15. Forterre,P. (2002) A hot story from comparative genomics: reverse gyrase is the only hyperthermophile-specific protein. *Trends Genet*., **18**, 236–237.
16. Rodriguez,A.C. (2002) Studies of a positive supercoiling machine. Nucleotide hydrolysis and a multifunctional ''latch'' in the mechanism of reverse gyrase. *J. Biol. Chem*., **277**, 29865–29873.
17. Matoba,K., Mayanagi,K., Nakasu,S., Kikuchi,A. and Morikawa,K. (2002) Three-dimensional electron microscopy of the reverse gyrase from *Sulfolobus tokodaii*. *Biochem. Biophys. Res. Commun*., **297**, 749–755.
18. Stasiak,A. and Di Capua,E. (1982) The helicity of DNA in complexes with recA protein. *Nature*, **299**, 185–186.
19. McDonald,M.R. and Kaufmann,B.P. (1954) The degradation by ribonuclease of substrates other than ribonucleic acid. *J. Histochem. Cytochem*., **2**, 387.
20. Changela,A., DiGate,R.J. and Mondragon,A. (2001) Crystal structure of a complex of a type IA DNA topoisomerase with a single-stranded DNA molecule. *Nature*, **411**, 1077–1081.
21. Rodriguez,A.C. and Stock,D. (2002) Crystal structure of reverse gyrase: insights into the positive supercoiling of DNA. *EMBO J*., **21**, 418–426.
22. Machius,M., Henry,L., Palnitkar,M. and Deisenhofer,J. (1999) Crystal structure of the DNA nucleotide excision repair enzyme UvrB from *Thermus thermophilus*. *Proc. Natl Acad. Sci. USA*, **96**, 11717–11722.
23. Theis,K., Chen,P.J., Skorvaga,M., Van Houten,B. and Kisker,C. (1999) Crystal structure of UvrB, a DNA helicase adapted for nucleotide excision repair. *EMBO J*., **18**, 6899–6907.
24. Nakagawa,N., Sugahara,M., Masui,R., Kato,R., Fukuyama,K. and Kuramitsu,S. (1999) Crystal structure of *Thermus thermophilus* HB8 UvrB protein, a key enzyme of nucleotide excision repair. *J. Biochem. (Tokyo)*, **126**, 986–990.
25. Moolenaar,G.F., Hoglund,L. and Goosen,N. (2001) Clue to damage recognition by UvrB: residues in the beta-hairpin structure prevent binding to non-damaged DNA. *EMBO J*., **20**, 6140–6149.
26. Skorvaga,M., Theis,K., Mandavilli,B.S., Kisker,C. and Van Houten,B. (2002) The beta-hairpin motif of UvrB is essential for DNA binding, damage processing, and UvrC-mediated incisions. *J. Biol. Chem*., **277**, 1553–1559.
27. Doetsch,P.W. and Cunningham,R.P. (1990) The enzymology of apurinic/apyrimidinic endonucleases. *Mutat. Res*., **236**, 173–201.
28. Chu,G. (1997) Double strand break repair. *J. Biol. Chem*., **272**, 24097–24100.
29. Bell,S.D., Jaxel,C., Nadal,M., Kosa,P.F. and Jackson,S.P. (1998) Temperature, template topology, and factor requirements of archaeal transcription. *Proc. Natl Acad. Sci. USA*, **95**, 15218–15222.
30. Lopez-Garcia,P. and Forterre,P. (1999) Control of DNA topology during thermal stress in hyperthermophilic archaea: DNA topoisomerase levels, activities and induced thermotolerance during heat and cold shock in Sulfolobus. *Mol. Microbiol*., **33**, 766–777.
31. Wang,C.C. and Tsou,C.L. (1998) Enzymes as chaperones and chaperones as enzymes. *FEBS Lett*., **425**, 382–384.
32. Gangloff,S., McDonald,J.P., Bendixen,C., Arthur,L. and Rothstein,R. (1994) The yeast type I topoisomerase Top3 interacts with Sgs1, a DNA helicase homolog: a potential eukaryotic reverse gyrase. *Mol. Cell. Biol*., **14**, 8391–8398.